PHYSICAL REVIEW B VOLUME 14, NUMBER 7 1 OCTOBER 1976

Study of the rare-earth–oxygen interaction in iron by lattice location and perturbed-angular-correlation experiments*

L. Thomé and H. Bernas
Institut de Physique Nucléaire, Université Paris-Sud, 91406-Orsay, France

F. Abel, M. Bruneaux, and C. Cohen
Groupe de Physique des Solides de l'Ecole Normale Supérieure, Université Paris-VII, 75005-Paris, France

J. Chaumont
Laboratoire René Bernas du C.S.N.S.M., 91406-Orsay, France
(Received 2 February 1976)

In a study of the rare-earth–oxygen interaction in iron, lattice location and integral perturbed-angular-correlation experiments were performed after implantation of Yb and ^{16}O in iron single crystals and foils. The ion-implantation energies were chosen so that the depth profiles overlapped almost completely. A strong Yb-O interaction is evidenced in both types of experiments. However, its effects on channeling results and on hyperfine-interaction measurements are found to be entirely different: In the present case, the usually assumed simple correspondence between impurity lattice location and hyperfine-field values certainly does not hold. The results are discussed in the light of a simple statistical model for the interaction probability between rare-earth and oxygen atoms.

I. INTRODUCTION

This report is the first part of several pieces of work[1-3] bearing on the relation between the hyperfine interaction (HFI) at the nucleus of heavy impurities implanted in iron and their lattice location, with an emphasis on the effect of implantation-induced radiation damage. The problem is discussed in detail in Ref. 2 in the light of work by other authors.[4-8] When these experiments were undertaken, the situation was the following. A Mössbauer experiment[6] had shown that after room-temperature ^{151}Gd implantation into Fe at 50 keV, approximately 60% of the implanted rare-earth (RE) ions experienced a single magnetic HFI, while about 40% had the HFI parameters observed in nonmagnetic Gd_2O_3. Since lattice-location results[9] had indicated in several cases that some 60% of implanted RE ions were definitely in substitutional sites, it was tempting to identify the magnetic HFI population with the substitutional RE atoms and the nonmagnetic HFI population with RE atoms in oxide form. The fact that integral perturbed-angular-correlations (IPAC) and lattice-location results for ^{169}Yb (^{169}Tm) showed a strong correlation upon annealing[1,7] lent further support to this simple picture: the annealing process apparently led to some interaction between the implanted RE atoms and the oxygen impurities introduced by previous metallurgical treatment and/or by recoil implantation from the surface oxide layer. As a result, the magnetic moment on the RE atom apparently disappeared and it lost its substitutional position. This interpretation was not corroborated however by several results. Mössbauer experiments on Er implanted in[10] Fe showed unequivocally that essentially 100% of the RE ions experienced the same magnetic HFI, quite close to the free-ion value. Other Mössbauer experiments on[11] Dy and more recently[12] Tm implanted in Fe showed no indication of the existence of a nonmagnetic RE oxide. The latter result confirmed a previous IPAC study of ^{169}Tm in Fe.[13] Lattice-location results showing the special role of the (100) plane in[1] Fe underlined the caution with which channeling results must be analyzed.[2] Last, the results of Ref. 8 demonstrated directly that if the implanted RE layer is deep enough, recoil implantation and/or diffusion from the surface oxide layer do not produce a significant increase of the oxygen concentration at the RE implantation depth in Fe.

In view of these results, the effect of the RE-O interaction on the HFI and channeling results remained unclear. In order to study the problem, we implanted both O and Yb into Fe single crystals or foils (at energies high enough to avoid surface oxide interference), *at the same depth* so as to favor the interaction between the RE and O atoms. The RE-impurity lattice location was measured before and after sample annealing, and the results compared to those obtained previously[1,2,7]; the RE-impurity HFI was also measured (before annealing) in IPAC experiments. A strong RE-O interaction is evidenced. We show that while this interaction *reduces* the lattice-location backscattering ratio (often identified with the "substitutional fraction"), it may simultaneously *increase* the magnetic HFI at room temperature. This re-

sult suggests that the assumption of a simple correspondence between the two quantities be critically re-examined. Qualitative explanations are suggested for the absolute values of the apparent substitutional fraction ϵ and the HFI; a very simple model, including the effect of trapping by irradiation-induced defects, is found to account quantitatively for the relative values of ϵ and the magnetic HFI, and suggests further experiments to study the corrosion properties of ion-implanted metals from a "microscopic" point of view.

II. EXPERIMENTAL

The samples used for the lattice-location experiments were (001)-oriented Fe single crystals annealed and electrochemically polished before implantation. The oxygen content of the remaining surface oxide layer was measured after polishing via the $^{16}O(d,p)^{17}O^*$ nuclear reaction, and found to be about 10^{16} at. cm^{-2} (corresponding to an oxide layer of ~30 Å assuming Fe_2O_3). The total bulk impurity content of these single crystals was approximately 500 ppm, with 20 ppm of oxygen. Such (rather high) values are standard for Fe single crystals. The samples used for the IPAC experiments were zone-refined Fe foils, thinned down to approximately 50 μm; their surface oxide layer was comparable to that of the single crystals, but their total impurity content was certainly less than 100 ppm. In view of the implanted-oxygen concentrations (see below), the difference in bulk oxygen content between the single crystals and the foils before implantation is not significant.

All the stable ion implantations were carried out with the Orsay ion implantor, whose equipment and performances have already been described.[14] As in previous work,[2] multiply charged ion beams were used when necessary, and Fe single crystals were oriented on a goniometer to ensure implantation in a random direction. The vacuum in the implantation chamber ($\lesssim 5\times10^{-7}$ Torr), provided by a turbomolecular pump, is devoid of residual organic vapor. Typical ion currents were ~100 nA cm^{-2} for O and stable Yb ion implantations. Radioactive ^{169}Yb was implanted at 130 keV with the Orsay high-resolution isotope separator,[15] using the same postaccelerating system as above; typical ion currents were 5 nA cm^{-2}, including contamination by neighboring stable ion beams (in all cases, the ion current was measured with an accuracy better than 10%, the contamination level was lower than 10%).

Tables I and II summarize the implantation conditions and results. An ^{174}Yb ion implanted at 80 keV has a projected range R_p of ~130 Å and a straggling width ΔR_p~40 Å; for a 130-keV ^{169}Yb ion, R_p~190 Å and ΔR_p~60 Å; for a 400-keV ^{174}Yb ion, R_p~520 Å and ΔR_p~170 Å.[16] For samples S1–S4 and R1–R3, the Yb implantation was preceded or followed by an ^{16}O implantation; the O-implantation energy was selected in order to ensure a maximum overlap (essentially 100%) of the Yb- and O-implantation profiles. Annealing of samples S3, S6, and S9 was performed in a vacuum better than 2×10^{-7} Torr, provided by an ion pump and a liquid-nitrogen vapor trap. All anneals lasted 15 min. The oxide layer measured on several samples was again found to be $\lesssim$30 Å.

The channeling experiments were carried out at the 2-MeV Van de Graaff accelerator of the Ecole Normale Supérieure with a 1.8-MeV ^{14}N ion beam using the setup described in Ref. 17. The experimental conditions were identical to those used previously[2]; the rather poor energy resolution [75 keV full width at half-maximum (FWHM)], due to the fast electronics used in order to avoid pileup

TABLE I. Compilation of lattice-location results on Fe implanted with Yb or both Yb and oxygen. The parameter ϵ is the RBS extinction ratio (see text), while $l_{1/2}$ is the FWHM of the angular scan for Fe or Yb measured under the conditions described for ϵ (see text).

Sample	Implanted species and dose (at. cm^{-2})	Implantation energy (keV) Yb	O	Annealing temperature	ϵ	ϵ(100)	$l_{1/2}$(Fe)	$l_{1/2}$(Yb)
S-1 [a]	5×10^{14}(Yb) + 5×10^{14}(O)	400	44	RT	0.42(3)	0.42(2)	3.2 deg	3.2 deg
S-2 [a]	5×10^{14}(O) + 5×10^{14}(Yb)	400	44	RT	0.41(3)			
S-3	5×10^{14}(O) + 5×10^{14}(Yb)	400	44	300 °C	0.35(3)		3.2 deg	3.1 deg
S-4	2×10^{15}(O) + 5×10^{14}(Yb)	400	44	RT	0.18(3)	0.32(4)		
S-5	5×10^{14}(Yb)	400		RT	0.56(3)	0.56(4)		
S-6	5×10^{14}(Yb)	400		300 °C	0.56(3)	0.56(4)		
S-7 [b]	2×10^{14}(Yb)	80		RT	0.58(4)			
S-8 [b]	2×10^{14}(Yb)	80		300 °C	0.31(4)			
S-9 [c]	5×10^{14}(Yb)	80		300 °C	0.43(4)		3.2 deg	2.9 deg

[a] Samples S-1 and S-2 are identical except in the sequence of implantations.

[b] Samples S-7 and S-8 are results taken from the work of Alexander *et al.* (Ref. 7).

[c] Some indication of a flux-peaking effect was found in this angular scan: see Fig. 2. This is in agreement with Ref. 7.

TABLE II. Integral perturbed angular correlation results for Fe implanted with ^{169}Yb and oxygen.

Sample	Implanted species and dose (at. cm^{-2})	Implantation energy (keV) Yb	O	A [a] $\frac{5}{2}$ level	$\frac{7}{2}$ level	$\Delta\theta$ (mrad) [b] $\frac{5}{2}$ level	$\frac{7}{2}$ level
R-1	5×10^{12}(Yb) + 10^{14}(O)	130	12	0.219(4) [c]	0.095(3)	192(10)	52(10)
R-2	5×10^{12}(Yb) + 5×10^{14}(O)						
R-3	3×10^{14}(Yb) + 3×10^{14}(O)			0.330(10)	0.093(8)	174(15)	227(15)

[a] A is the measured anisotropy of the angular correlations (see text).
[b] $\Delta\theta$ is the measured rotation of the angular correlations (see text).
[c] The values in parentheses in the last four columns are the experimental errors.

effects, corresponds to a depth resolution of ~200 Å for Yb in Fe at a laboratory detection angle of 165 deg.

The integral perturbed-angular-correlation (IPAC) experiments were performed on the ^{169}Tm daughter of ^{169}Yb implanted at room temperature into Fe foils which had previously been submitted to ^{16}O implantation. Here again, the Yb and O distributions overlap. The IPAC measurements were carried out simultaneously on the 118-keV (90 psec) and 139-keV (450 psec) states of ^{169}Tm, as in Refs. 3 and 13: a Ge(Li) detector was used throughout and angular correlation curves were measured for both cascades, as shown in Fig. 3. All of these IPAC measurements were carried out at room temperature (this is an important point in the discussion of Sec. III B).

III. RESULTS AND DISCUSSION

A. Lattice-location experiments

Rutherford backscattering (RBS) spectra were taken with samples aligned along the [100] axis and, in a number of cases, along the [111] and [110] axes as well as the (100) and (110) planes, in an attempt to precisely determine the nonsubstitutional-impurity lattice location. Typical [100]-aligned spectra and the corresponding random spectra are shown in Fig. 1. The parameter of interest is the corrected impurity-extinction ratio defined as $\epsilon = [1-\chi_{Yb}][1-\chi_{Fe}]^{-1}$, where χ is the usual ratio of backscattering yields for an aligned and the corresponding random spectrum.[9]

When RBS spectra were taken along different directions for a sample, the value of ϵ was found to be identical for all the axes and planes studied, with the exception in several cases of the (100) plane. This planar effect will be discussed later. Angular scans across the [100] axis were also recorded, both on the Yb impurity and on the Fe host (Fig. 2). The FWHM of the Yb dips was found to be equal to (or slightly narrower than) the corresponding Fe dips. For these measurements, as well as for the measurements of ϵ, the value of

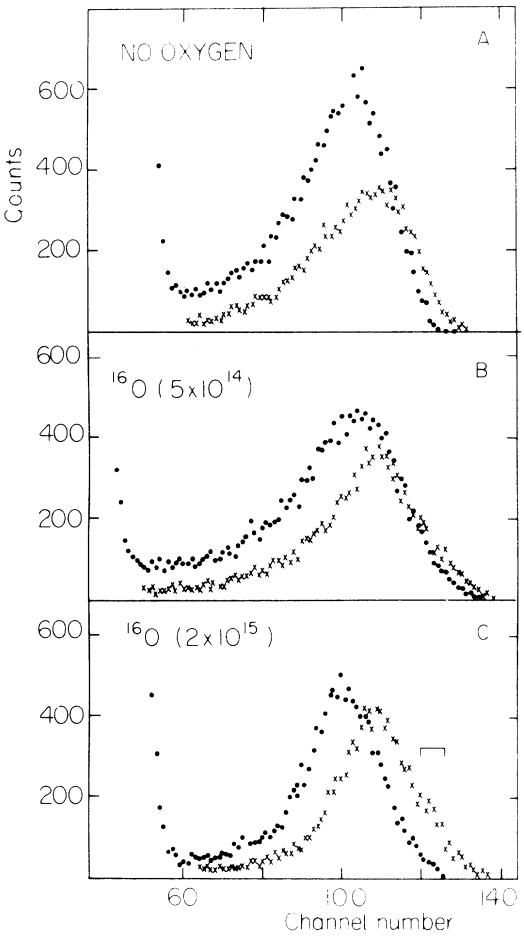

FIG. 1. Experimental Rutherford backscattering spectra for 400-keV Yb-implanted Fe, with and without oxygen implantation at the Yb penetration depth. Only the high-energy portion of the spectra is shown (i.e., RBS from implanted Yb). Full circles indicate RBS spectra in random direction; crosses indicate RBS spectra along [100] axis. Curve A: sample S-5. Curve B: sample S-1. Curve C: sample S-4. For clarity, in curve C, the "random" spectrum has been shifted towards the left as indicated in the figure. The count rates for all spectra were typically 2×10^4 counts/sec.

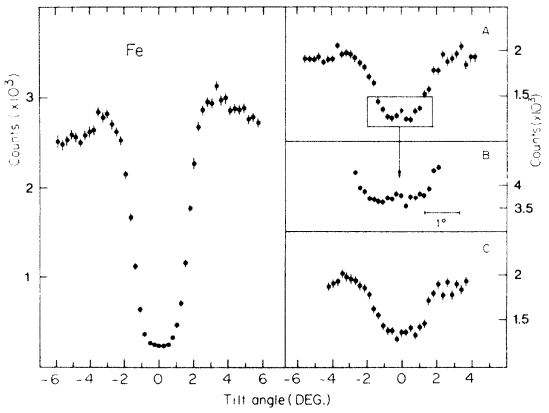

FIG. 2. Typical angular scans across the [100] axis for the Fe host (sample S-1) and the Yb impurity (curves *A* and *B*: sample S-1; curve C: sample S-3). Curve *B* is a scan across the bottom of the dip measured in *A*, with improved statistics (note the change in horizontal scale).

χ_{Yb} was obtained by integrating all the counts in the Yb peak of the RBS spectrum, and the value of χ_{Fe} was obtained by integrating the counts in the portion of the Fe RBS spectrum corresponding to the Yb penetration depth and range straggling. Some indication of a flux-peaking effect was found (sample S1) in only one case.

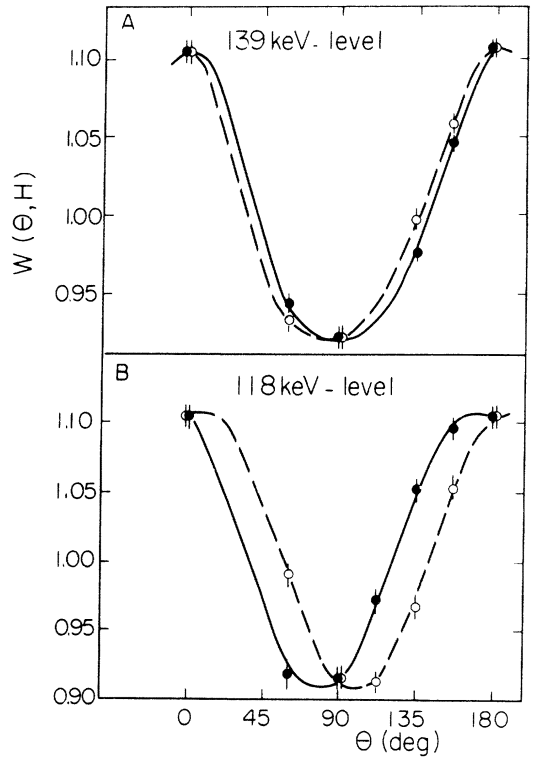

FIG. 3. Integral perturbed-angular-correlation curves of the 177–131-keV (*A*) and 198–110-keV (*B*) γ cascades in ^{169}Tm for sample R-1 (essentially identical results were obtained for sample R-2). This is the case where $z \simeq 1$ (see text and *Note added in proof*).

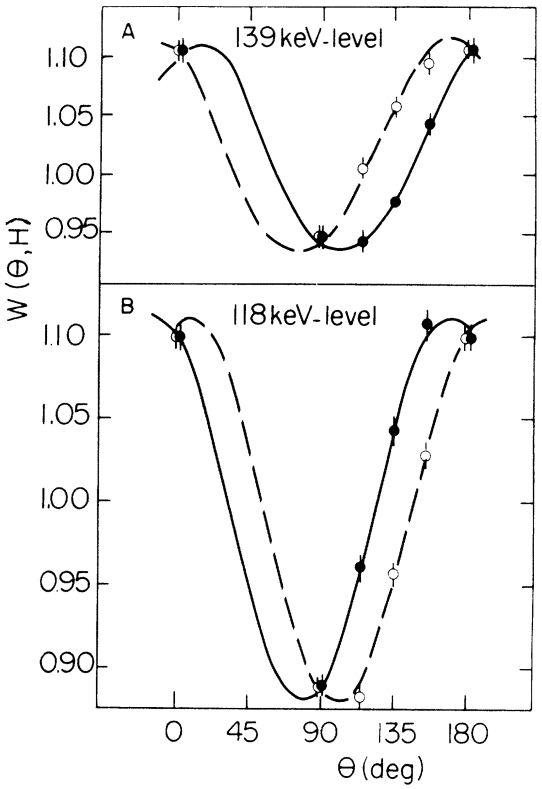

FIG. 4. Integral perturbed-angular-correlation curves of the 177–131-keV (*A*) and 198–110-keV (*B*) γ cascades in ^{169}Tm for sample R-3. This is the case where $z \simeq 0.25$ (see text and *Note added in proof*).

Typical Fe and Yb angular scans are presented in Fig. 2; the lattice-location results for all our samples are presented in Table I, which also summarizes the relevant results of other authors. The following conclusions may be drawn at this stage.

1. Ytterbium-implanted samples

(i) Comparison of samples S5 and S7 shows that the value of the corrected Yb extinction ratio ϵ is ~0.57 both at 80-keV and 400-keV implantation energies. We have previously demonstrated[8] that no internal oxidation takes place in the latter case; the present results show that as long as no annealing above room temperature occurs, ϵ is not significantly affected by internal oxidation in either case. This contradicts the interpretation of Refs. 6 and 7.

(ii) The annealing-temperature dependence of ϵ depends on the implantation energy (compare samples S6, S8, and S9): annealing up to 300 °C has essentially no effect on a 400-keV Yb-implanted sample, while it reduces ϵ from 0.58 to 0.35

(this work) or[7] 0.31 for an 80-keV Yb-implanted sample. This result suggests that oxygen diffusion from the nearby surface oxide may induce a RE-O interaction affecting ϵ for low-energy implanted samples (the Yb-ion-implantation profile at 80 keV is centered at ~130 Å with a FWHM of ~80 Å, while typical surface oxide layers vary from ~30 to ~50 Å).

2. *Ytterbium plus oxygen-implanted samples*

(i) When O is implanted at the Yb implantation depth and no annealing is performed, ϵ is reduced; the higher the oxygen dose, the lower the value of ϵ for a given Yb dose. The variation of ϵ does not depend on the sequence of the O and Yb implantations (compare S1 and S2).

(ii) Upon annealing at 300 °C, the value of ϵ is further reduced for these samples: the Yb-O interaction is enhanced by annealing. This confirms our explanation of the reduction in ϵ for low-energy Yb-implanted iron (samples S8 and S9) after annealing at 300 °C.

(iii) When O is implanted at high dose (sample S4), the value of ϵ in the (100) plane is found to be almost double that of ϵ along the [100] axis. A similar result was obtained after annealing of Yb-implanted Fe.[1,2] In that case, it was attributed to the interaction between Yb atoms and vacancy loops formed in the (100) plane. Here, we may surmise that the Yb-O interaction takes place in the (100) plane: whether this is related to an effect of the vacancy loops is open to question.

B. Hyperfine-interaction experiments

Integral perturbed-angular-correlation (IPAC) experiments were carried out on three samples for which only the relative concentrations of Yb and O were changed: Table II lists our implantation conditions and results. Complete angular correlations were measured, as shown in Figs. 3 and 4. The anisotropy A in Table II is defined, as usual,

$$A = [W(\pi) - W(\tfrac{1}{2}\pi)]/W(\tfrac{1}{2}\pi) .$$

Its relation to the attenuation coefficient of the perturbed angular correlation depends on the interactions which are assumed to be present. The same is true of the rotation $\Delta\theta$ of the perturbed-angular-correlation pattern in an external magnetic field.[18] In all cases, IPAC experiments only provide a bulk average over impurity nuclei with possibly different HFI amplitudes. It is clear that more precise information would be obtained from a Mössbauer experiment on the 8.4-keV level of ^{169}Tm, if the number of sites with different magnetic and quadrupolar HFI was sufficiently small to benefit from the resolution of the method. We have already discussed the possibilities and shortcomings of IPAC measurements in experiments such as these, and the advantage of simultaneously measuring the IPAC of two different nuclear levels in the ^{169}Tm isotope.[3,13] Bearing this in mind, it is possible to perform a self-consistent analysis of the data which provides interesting information on the variations of the HFI upon oxygen implantation.

Our results on room-temperature implanted ^{169}Yb in Fe were consistent with the assumption that a fraction f of the ^{169}Tm nuclei experienced a time-dependent magnetic HFI, while a fraction $(1-f)$ was not affected by any HFI at all. Hence the measured angular correlation was

$$W_{\text{meas}}(\theta) = f\,W_{\text{pert}}(\theta) + (1-f)\,W_{\text{unpert}}(\theta) . \qquad (1)$$

The situation in which $f=1$ was studied in Ref. 13; other experiments[1,7] were also interpreted with Eq. (1). Here, in order to account for the variations of the anisotropy and rotation of both angular correlations (Table II), it is necessary to introduce a different interaction. The simplest is the assumption of a combined [(magnetic dipole) + (electric quadrupole)] interaction affecting *all* the ^{169}Tm nuclei. In order to reduce the number of free parameters in the analysis, we have also assumed that this is a static interaction: any time dependence would introduce comparatively small corrections to the parameters deduced from the experiments. The angular correlation attenuation coefficient which describes this interaction may be obtained[19,20] from the general theory:

$$G^{NN}_{k_1k_2}(x,y) = \frac{[(2k_1+1)(2k_2+1)]^{1/2}}{2(2I+1)} \times [a^N_{k_1k_2}(x,y) + i\,b^N_{k_1k_2}(x,y)]$$

(using the standard notations of Ref. 18, in which $x=\omega_Q\tau_N$ and $y=\omega_B/\omega_Q$, where ω_Q and ω_B are the frequencies corresponding to the quadrupolar and magnetic parts of the interaction, respectively, and τ_N is the lifetime of the intermediate nuclear level. The coefficients $a^N_{k_1k_2}$ and $b^N_{k_1k_2}$ are defined and tabulated for various values of x and y in Ref. 20. Comparison of the experimental attenuation coefficients with those deduced from the tables provides sets of values of ω_Q and ω_B; when two different levels are compared in the same nucleus, the ratio y is unaffected but x is different, so that a further constraint is set on the possible values of ω_Q and ω_B. For samples R1 and R2, the experimental values (Table II) pertaining to the $\frac{5}{2}$ level lead to two very different sets of HFI frequencies, one of which corresponds to an almost pure magnetic interaction while the other corresponds to a strong quadrupolar term. The experimental values

of A and $\Delta\theta$ obtained for the $\frac{7}{2}$ level rule out the former case and are consistent with the latter. Because of the uncertainties in the IPAC analysis, no attempt was made to obtain a better fit to the results. From the results on the $\frac{5}{2}$ level, the following values may be deduced:

$$\omega_B = (6.5\pm2.5)\times10^3 \text{ MHz},$$

$$\omega_Q = (1.7\pm0.6)\times10^3 \text{ MHz},$$

in which the error bars include all the estimated uncertainties. This leads to an average magnetic hyperfine field $H_{hf} = 4.5\pm1.5$ MOe at the ^{169}Tm nucleus, compared to the hyperfine field $H_{hf} = 1.75 \pm 0.3$ MOe obtained for a room-temperature implanted FeYb without annealing or oxygen implantation. The assumption that, in these samples, all the ^{169}Tm nuclei experience the same HFI will be justified in Sec. IV.

When the Yb and O concentrations are equal (sample R3), the values reported in Table II are much nearer to those of Ref. 13. These results will be discussed in Sec. IV B.

IV. INTERPRETATION

For the concentration ranges involved in experiments S1–S6, the average distance between a RE and an oxygen is about ten interatomic distances. Previous work has shown[1,2] that Yb is not mobile at least up to 500 °C in Fe, so we will assume that oxygen atoms must move for the RE-O interaction to take place and that the migrating O may be captured either by a RE atom or by a defect cluster. It is known that the number of implantation-induced defect clusters is proportional to the implantation dose; this was checked in the case of Yb in Fe, and the clusters were identified as vacancy loops.[21] For the sake of simplicity, we assume that the number of O atoms that may be trapped by a defect cluster is not restricted, while the number of O atoms trapped by a RE is at most one. The latter two assumptions could be modified if necessary, particularly if other traps were found to be effective. If N_0 is the number of implanted oxygen ions, N_{Yb} the number of implanted Yb ions, and z is the fraction of RE atoms which have trapped a migrating oxygen atom, the application of elementary statistics to the capture process provides the following relation:

$$z - \alpha \ln(1-z) = N_0/N_{Yb}\,, \tag{2}$$

where $\alpha = (N_C/N_{Yb})(\sigma_C/\sigma_{Yb})$ is a coefficient in which N_C is the number of defect clusters, σ_C is the trapping cross section of an oxygen atom by a defect cluster, and σ_{Yb} the trapping cross section by an Yb atom. When z is close to unity, Eq. (2) becomes

$$z = 1 - \exp(-N_0/\alpha N_{Yb})\,, \tag{3}$$

while for small values of z, we have

$$z = N_0/(1+\alpha)N_{Yb}\,. \tag{4}$$

A plot of z as a function of N_0/N_{Yb} is shown in Fig. 5.

This very simple model predicts the fraction z of the implanted Yb ions which interact with oxygen atoms. It does not provide any information on the effect of the interaction on the measured parameter (i.e., ϵ or the HFI). We shall discuss the two measurements in turn.

A. Lattice location

Assuming that (i) the trapping cross section σ_{Yb} of an Yb atom is independent of its lattice site, and (ii) when a substitutional Yb atom traps an oxygen atom it is displaced and appears as random [except in the (100) plane], the fraction z is simply

$$z = (\epsilon_i - \epsilon_f)/\epsilon_i\,, \tag{5}$$

where ϵ_i and ϵ_f are the values of ϵ measured before and after the oxygen implantation. The value of α may be deduced by comparing Eqs. (2) and (5) for a given sample: e.g., in the case of sample S1, we find $\alpha = 2.6$. With this value of α, the predicted value of ϵ for sample S4 is 0.16, in very good agreement with the experimental value of 0.18. No assumption is made (and no information is obtained) on the reasons for which ϵ_i is not unity: our discussion only concerns the *reduction* in ϵ. According to this model, the variation of ϵ upon annealing is related to the temperature dependence of α. Electron microscopy results show that the number of defect clusters decreases upon

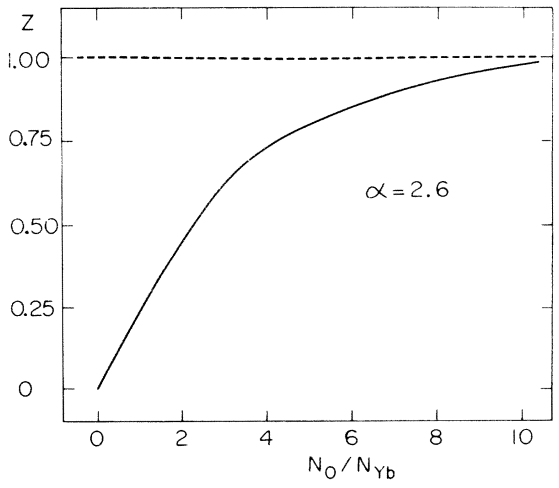

FIG. 5. Fraction z of the rare-earth atoms which have trapped an oxygen atom, according to Eq. (2), with the parameter $\alpha = 2.6$. For discussion, see text.

annealing, with some clusters growing at the expense of others.[22] Since σ_{Yb} and N_{Yb} are not temperature dependent, our results indicate that any increase in σ_C is more than compensated by the reduction in N_C: two small clusters are more efficient than a single large one in trapping oxygen.

Our angular scans do not provide enough information to discuss the geometry of the Yb-O interaction, and the possible role of lattice defects is unknown. However, the fact that this interaction displaces the Yb clearly indicates that the trapped oxygen atom must be very close to the RE impurity.

B. Hyperfine interactions

Using the value $\alpha = 2.6$ deduced from the lattice-location results, we may calculate z for the HFI experiments in Table II. For samples R1 and R2, z is essentially unity (this is corroborated by the fact that the measured HFI is the same in spite of a fivefold difference in oxygen concentrations). For sample R3, z is approximately 0.25. We can thus expect differences in the nature and in the amplitude of the RE-O interaction between these two sets of samples: the HFI proves to be very sensitive to these differences.

When $z = 1$, the very large apparent increase in the magnetic term of the HFI, as well as the existence of a strong quadrupolar contribution (corresponding to an electric field gradient of $\sim 7 \times 10^{18}$ V/cm^2) in the oxygen-implanted samples could very well be due to the crystal field set up by the oxygen atoms neighboring the Tm^{3+} ions. It is well known that the temperature dependence of the HFI depends on the relative strength of the magnetic term and of the crystal-field potential in the hyperfine Hamiltonian.[13] If the two terms are of the same order of magnitude, the temperature variation is often rather flat and the HFI at $T = 0$ is typically $\sim 50\%$ of the free-ion value, due to the averaging of the orbital moment over several crystal-field representations. Thus, compared to the value previously measured for $Fe^{169}Yb$,[13] the magnetic hyperfine field for the oxygen-implanted sample may be *larger* at room temperature, and significantly *smaller* at 4.2 K.

We have seen that if $z = 1$, all the RE atoms have an O atom in their immediate vicinity. The identical HFI parameters obtained from samples R1 and R2 indicate that the crystal-field terms are concentration independent in this case—hence that the immediate surroundings of all RE atoms are identical in each of these two samples (i.e., the RE-O interaction has a well-defined geometry). This is consistent with the analysis of Sec. III B.

When 25% of the RE atoms have trapped oxygen (sample R3), the situation is far more complicated. We may surmise that the RE-O interaction is the same as above for those 25%, but that the remaining Yb atoms have statistically different surroundings. The simplest hypothesis would be that these Yb atoms are sufficiently far from the trapped oxygen atoms to produce a *Fe*Yb dilute alloy, for which the HFI was measured in Ref. 13: Eq. (1) could then be used, with $f = 0.25$, to deduce the measured angular correlation. Using the results of Sec. III B and those of Ref. 13, we find that the experimental values for sample R3 can be reproduced in this way to within about 10%. Of course, although this result is plausible, a more complicated distribution of the noninteracting Yb atoms cannot be excluded: a study of the various possible components in the HFI was beyond the scope of this work.

V. CONCLUSION

Our results clearly establish that when oxygen is present in the RE implantation layer, a strong RE-O interaction takes place. We have shown that the effect of this interaction on the RE lattice location and on its HFI are entirely different: the RBS extinction ratio ϵ and the HFI at the ^{169}Tm nucleus can even vary in opposite directions when the oxygen concentration increases. A simple statistical model, assuming defect-induced mobility of O and its trapping by Yb or defect clusters, accounts for the lattice location results insofar as relative changes in ϵ are concerned. It is consistent with the HFI results, if the latter are determined by the setting up of a strong crystal-field potential when oxygen is introduced in the neighborhood of ^{169}Tm. The results are found to depend strongly on the relative concentrations of RE and oxygen, and also on the implantation energy. This probably accounts for the discrepancy between the results of Refs. 1 and 7, since the low implantation energy used in Ref. 7 may favor the RE-oxygen interaction by producing large defect concentrations—hence oxygen mobility—at the interface between the surface oxide layer and the bulk iron. The present experiments provide an example of a situation in which HFI and lattice-location results bear no simple relation. Other cases have been found, particularly after high-temperature implantation[2]: radiation damage then seems to play an important role.

Note added in proof. A drawing error was made

in Figs. 3 and 4. In both of these figures, the solid line in *A* and the dashed line in *B* correspond to "field up"; the dashed line in *A* and the solid line in *B* correspond to "field down" in the standard terminology of IPAC measurements (Ref. 18).

ACKNOWLEDGMENTS

We wish to thank F. Lalu, R. Meunier, G. Moroy, and M. Salomé, as well as E. d'Artemare and E. Girard for their valuable technical assistance.

*Work supported by C.N.R.S. under Contract Nos. RCP-157 and RCP-185.

[1]F. Abel, M. Bruneaux, C. Cohen, H. Bernas, J. Chaumont, and L. Thomé, Solid State Commun. 13, 113 (1973); in *Applications of Ions Beams to Metals*, edited by S. T. Picraux, E. Eer Nisse, and F. Vook (Plenum, New York, 1974), p. 377.

[2]L. Thomé, F. Abel, M. Bruneaux, J. Chaumont, C. Cohen, and H. Bernas (unpublished).

[3]L. Thomé and H. Bernas (unpublished).

[4]H. de Waard and L. C. Feldman, in *Applications of Ions Beams to Metals*, edited by S. T. Picraux, E. Eer Nisse, and F. Vook (Plenum, New York, 1974), p. 317.

[5]H. de Waard, Phys. Scr. 11, 157 (1975), and references therein.

[6]R. L. Cohen, G. Beyer, and B. I. Deutch, Phys. Rev. Lett. 33, 518 (1974).

[7]R. Alexander, E. Ansaldo, B. I. Deutch, J. Gellert, and L. C. Feldman, Ref. 4, p. 365.

[8]L. Thomé, H. Bernas, J. Chaumont, F. Abel, M. Bruneaux, and C. Cohen, Phys. Lett. A 54, 37 (1975).

[9]For a review, see S. T. Picraux, in *New Uses of Ion Accelerators*, edited by J. S. Ziegler (Plenum, New York, 1975), p. 229.

[10]L. Niesen and P. J. Kikkert, *Hyperfine Interactions in Nuclear Reaction and Decay* (Uppsala U.P., Uppsala, 1974), p. 160.

[11]P. Inia, Ph.D. thesis (University of Groningen, 1973) (unpublished); P. Inia and H. de Waard, in *Angular Correlations in Nuclear Decay*, edited by H. Krugten and B. Van Nooijen (Rotterdam U.P., Rotterdam, 1973), p. 371.

[12]H. P. Wit and L. Niesen, in *International Conference on Hyperfine Interactions, Leuven, 1975* (unpublished).

[13]H. Bernas and H. Gabriel, Phys. Rev. B 7, 468 (1973).

[14]J. Chaumont, F. Lalu, M. Salomé, H. Bernas, and L. Thomé, Le Vide, Suppl. Vol. 171, p. 108, 1974.

[15]J. Camplan, R. Meunier, and J. L. Sarrouy, Nucl. Instrum. Methods 84, 37 (1970); and K. Alexandre, J. Camplan, M. Ligonnière, R. Meunier, J. L. Sarrouy, H. J. Smith, and B. Vassent, *ibid.* 84, 45 (1970).

[16]K. B. Winterbon, P. Sigmund, and J. B. Sanders, K. Dan. Vidensk. Selsk. Mat. Fys. Medd. 37, No. 14 (1970).

[17]G. Amsel, J. P. Nadai, E. d'Artemare, D. David, E. Girard, and J. Moulin, Nucl. Instrum. Methods 92, 481 (1971).

[18]H. Frauenfelder and R. M. Steffen, in α- β- and γ-*Ray Spectroscopy*, edited by K. Siegbahn (North-Holland, Amsterdam, 1965), p. 1101.

[19]K. Alder, H. Albers-Schönberg, E. Heer, and T. B. Novey, Helv. Phys. Acta 26, 761 (1953).

[20]R. M. Steffen, E. Matthias, and W. Schneider, USAEC report No. TID-17089, Part II (1962) (unpublished).

[21]H. Bernas, M. O. Ruault, and B. Jouffrey, Phys. Rev. Lett. 27, 859 (1971); see H. Bernas [Phys. Scr. 11, 167 (1975)] for a discussion of the relation between electron microscopy, lattice location, and HFI results.

[22]For a review of electron microscopy experiments on implanted metals, see M. Wilkens, in *Applications of Ions Beams to Metals*, edited by S. T. Picraux, E. Eer Nisse, and F. Vook (Plenum, New York, 1974), p. 441.